

# Er- and Eu-doped GaP-oxide porous composites for optoelectronic applications

L. Sirbu<sup>1</sup>, V. V. Ursaki<sup>1,2</sup>, I. M. Tiginyanu<sup>1,2</sup>, Ksenia Dolgaleva<sup>3</sup>, and Robert W. Boyd<sup>3</sup>

<sup>1</sup> National Center for Material Study and Testing, Technical University of Moldova, 2004 Chisinau, Moldova

<sup>2</sup> Laboratory of Low-Dimensional Semiconductor Structures, Institute of Applied Physics, Academy of Sciences of Moldova, 2028 Chisinau, Moldova

<sup>3</sup> Institute of Optics, University of Rochester, Rochester, New York 14627, USA

Received 17 August 2006, revised 2 September 2006, accepted 7 September 2006

Published online 8 September 2006

PACS 61.10.Nz, 61.43.Gt, 78.55.Mb, 81.05.Rm

\* Corresponding author: e-mail ursaki@yahoo.com, Phone: +373 22 237508, Fax: +373 22 319305

We demonstrate the controlled preparation of Er- and Eu-doped GaP-oxide porous composites. The fabrication procedure entails the use of porous semiconductor templates and the impregnation of rare earth ions from a rare earth salt solution in alcohol and thermal treatment. The composites exhibit

strong green and red emission that comes from finely dispersed ErPO<sub>4</sub> and EuPO<sub>4</sub> oxide submicron phases in the composite. These materials may prove useful in future generations of optoelectronic and photonic devices.

© 2007 WILEY-VCH Verlag GmbH & Co. KGaA, Weinheim

**1 Introduction** A great deal of research efforts are directed nowadays towards the development of random lasers based on disordered medium. Recently, Cao [1] reported a lasing process in highly disordered semiconductor nanostructures. The stimulated emission in a random laser may come either from near-bandgap electronic effects (exciton–exciton scattering or electron–hole plasma) as in the case of lasers based on ZnO compounds, or from transition metal and rare earth elements doped into the radiation emitting and amplifying phase.

Most of the random lasers demonstrated to date are based on powders, microspheres, nanocrystallite clusters, polycrystalline films, or disordered organic materials. However, these lasers are not suitable for integration with other optical or electronic functions. Composite materials prepared from porous semiconductor templates offer greater possibilities in this regard. Porous GaP networks are the most promising ones due to their strong photonic properties [2]. It has been demonstrated that macroporous gallium phosphide filled with air has the highest scattering efficiency among the known materials, due to the high refractive index of the bulk GaP.

Recently, an attempt was undertaken to dope a porous GaP template with an Eu impurity [3]. It was supposed that the observed strong visible emission comes from Eu<sup>3+</sup> ions incorporated into the porous GaP host. However, it is well known that rare earth ions are rarely if ever found at the tetrahedrally coordinated sites of a III–V host because of their large ionic radii [4]. Rare earth ions prefer a coordination number higher than six. It was demonstrated that the presence of oxygen is imperative for achieving efficient emission from rare earth ions introduced into a III–V material [5]. The oxygen co-doping leads to the formation of quasi-molecular centers at low impurity density [4, 5] and to the segregation of an oxide phase at higher doping levels [6].

In this letter, we identify the nano-phases and the electronic transitions responsible for the strong visible emission from nanocomposites prepared from porous GaP templates doped with Eu and Er lanthanides and propose a new approach for the design of multiphase random media based on porous semiconductor templates.

**2 Experimental details** (100)-oriented n-GaP:S wafers cut from Czochralski-grown ingots were used for the

fabrication of porous GaP layers. The anodic etching was carried out in a double-chamber electrochemical cell as described elsewhere [3].  $\text{Eu}^{3+}$  and  $\text{Er}^{3+}$  ions were incorporated into the porous GaP layer from  $\text{EuCl}_3 \cdot \text{C}_2\text{H}_5\text{OH}$  and  $\text{ErCl}_3 \cdot \text{C}_2\text{H}_5\text{OH}$  solutions, respectively. Afterwards, the samples were annealed using a halogen lamp heater for time periods ranging from several minutes to several hours at temperatures in the range of 500 to 1000 °C.

Photoluminescence (PL) was excited by different lines of an  $\text{Ar}^+$  laser and was analyzed by means of a double spectrometer having a resolution better than 0.5 meV. The samples were mounted on the cold station of a LTS-22-C-330 cryostat. In addition, X-ray diffraction (XRD) analysis of the samples was performed with a Philips X-Pert MPD System with  $\text{Cu K}\alpha_1$  radiation. The morphology and chemical composition microanalysis of anodically etched samples were studied using a TESCAN scanning electron microscope (SEM) equipped with an Oxford Instruments INCA energy dispersive X-ray (EDX) system.

### 3 Composition and structure characterization

The GaP templates used in this work consist of porous layers with pores stretching perpendicular to the sample surface to a depth of up to 100  $\mu\text{m}$  and with pore diameters and width of the porous skeleton walls of around 500 nm. The rare earth impurity introduced by impregnation into the templates was found to be optically activated at annealing temperatures higher than 700 °C, with higher temperatures producing a higher degree of activation. The annealing was performed in a nitrogen flow containing less than 1% oxygen. Under these conditions, the oxidation of the skeleton walls starts at around 600 °C, with higher anneal-

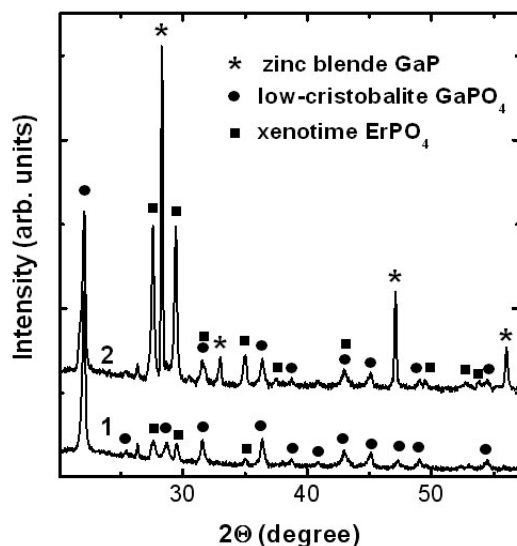


**Figure 1** XRD analysis of composites prepared on GaP templates infiltrated with an  $\text{ErCl}_3 \cdot \text{C}_2\text{H}_5\text{OH}$  solution with a concentration of 1 g/10 ml for 4 h and annealed at 900 °C for 30 min (curve 1) and, respectively, 1 g/2 ml, 4 h, 800 °C, 20 min (curve 2).

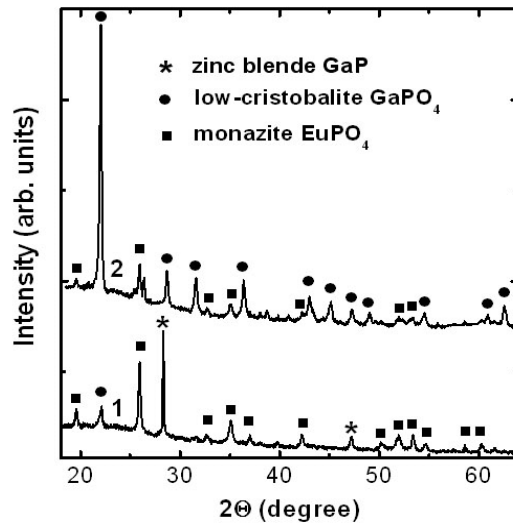


**Figure 2** XRD analysis of composites prepared on GaP templates infiltrated with an  $\text{EuCl}_3 \cdot \text{C}_2\text{H}_5\text{OH}$  solution with a concentration of 1 g/2 ml for 4 h and annealed at 800 °C for 10 min (curve 1) and, respectively, 1 g/5 ml, 4 h, 900 °C, 30 min (curve 2).

ing temperatures and longer durations of the treatment producing higher content of the oxide phase. At an annealing temperature of 900 °C the porous template is totally oxidized after 30 min of annealing. The EDX and RXD analyses of the oxide demonstrate the formation of a stoichiometric  $\text{GaPO}_4$  phase with the low-cristobalite (orthorhombic  $\text{C}222_1$ ) structure with tetrahedral coordination shells of oxygen atoms around both the gallium and phosphorus atoms.

As mentioned above, rare earth ions are large and are not well incorporated into the tetrahedrally coordinated sites of  $\text{GaPO}_4$  or in the zincblende GaP skeleton. More favourable is the segregation of the rare earth impurity in the form of finely dispersed nanophases in the composite. In order to identify these phases we have prepared samples with a high density of the Eu or Er impurity. We found that the constitution of the composite is controlled by the conditions of infiltration and annealing as illustrated in Figs. 1 and 2. Annealing at temperatures of up to 800 °C for 10 to 20 min results in the conservation of a significant part of the zincblende GaP skeleton (see curve 2 in Fig. 1 and curve 1 in Fig. 2). The other constituents of the composite are the native  $\text{GaPO}_4$  oxide and the  $\text{ErPO}_4$  or  $\text{EuPO}_4$  rare earth related oxides. The composite represents  $\text{ErPO}_4$  or  $\text{EuPO}_4$  micro-crystallites incorporated into the porous  $\text{GaPO}_4$  native oxide structure at annealing temperatures above 900 °C during more than 30 min (see curve 1 in Fig. 1 and curve 2 in Fig. 2). The density of the impurity can be controlled through the concentration of the infiltrated solution and the length of time that the samples are held in the solution before the thermal treatment.

The segregation at high densities of impurity rare-earth related phases were identified as tetragonal  $\text{I}4_1/\text{amd}$  xeno-

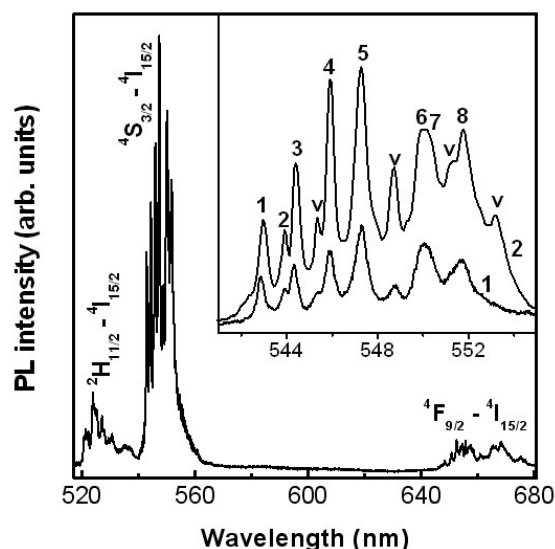


**Figure 3** PL spectrum of a sample doped with Er measured at room temperature. Inserted is the analysis of emission in the region of  $^4S_{3/2} \rightarrow ^4I_{15/2}$  transitions measured at room temperature (curve 1) and at 10 K (curve 2). The 8 lines resulting from the Stark splitting of the  $^4I_{15/2}$  multiplet manifold are labeled with digits. The lines labeled with “v” correspond to vibronic replicas.

time  $\text{ErPO}_4$  and monoclinic  $\text{P}_{21/n}$  monazite  $\text{EuPO}_4$ . Note that the coordination number for rare-earth ions is 8 and 9 in  $\text{ErPO}_4$  and  $\text{EuPO}_4$ , respectively. The sizes of crystallites deduced from the XRD spectra according to the Debye–Scherrer formula vary from several nanometers to more than 100 nm, depending on the conditions of fabrication. The scanning EDX analysis with the electron beam focused within a spot of 1  $\mu\text{m}$  shows a uniform distribution of  $\text{ErAsO}_4$  and  $\text{EuAsO}_4$  phases across the composite.

**4 Luminescence characterization** Analysis of the luminescence intensity under excitation by different laser lines shows that the highest luminescence intensity from samples doped with Er is observed under excitation by the 488.0 nm laser line, while in Eu doped samples this is achieved under the excitation by the 465.8 nm laser line. The fact that the quantum energy of these lines corresponds exactly to the  $^4F_{7/2} \leftarrow ^4I_{15/2}$  and  $^5D_2 \leftarrow ^7F_0$  transitions in  $\text{Er}^{3+}$  and  $\text{Eu}^{3+}$  ions, respectively, suggests that the excitation occurs via respective transitions, followed by non-radiative relaxation to the lower energy states  $^2H_{11/2}$ ,  $^4S_{3/2}$ , and  $^4F_{9/2}$  in  $\text{Er}^{3+}$  ions and  $^5D_0$  in  $\text{Eu}^{3+}$  ions. From these states, radiative transitions to the  $^4I_{15/2}$  ground state in Er and to  $^7F_{1-4}$  states in Eu occur.

Figures 3 and 4 illustrate the PL spectra of samples doped with Er and Eu ions, respectively. The correspondence of the Stark splitting of the ground  $^4I_{15/2}$  multiplet manifold of the  $\text{Er}^{3+}$  ion deduced from Fig. 3 to that previously measured in a xenotime  $\text{ErPO}_4$  [7] demonstrates that the green emission comes from the Er ions in this host. The spectrum in Fig. 4 coincides perfectly with that measured in a monazite  $\text{EuPO}_4$  [8].

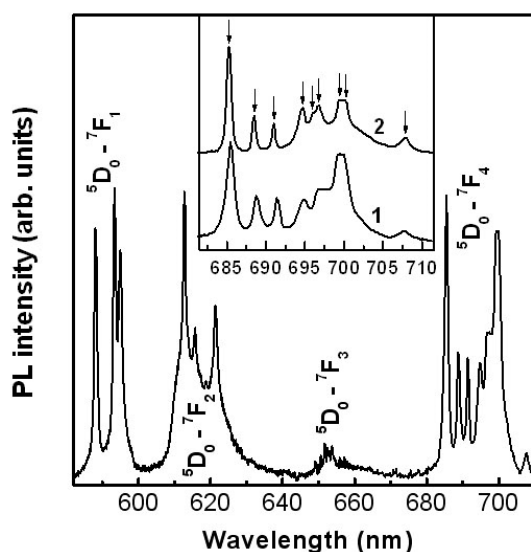


**Figure 4** PL spectrum of a sample doped with Eu measured at room temperature. Inserted is the analysis of emission in the region of  $^5D_0 \rightarrow ^7F_4$  transitions measured at room (curve 1) and 10 K (curve 2) temperatures. The arrows denote all the 9 lines resulting from the Stark splitting of the  $^7F_4$  multiplet manifold.

**5 Conclusions** The results of this work demonstrate the possibility of preparing in a controlled fashion a rare-earth-doped semiconductor-oxide porous composite. Possible applications include use as light emitters for integrated optoelectronic and photonic circuits. We also propose to utilize this composite in the design of multiphase random laser media in which the high-index semiconductor skeleton provides the strong light scattering necessary for the formation of random laser cavities, while the oxide rare-earth-doped phase plays the role of emitting and amplifying the electromagnetic radiation.

**Acknowledgements** This work was supported by U.S. CRDF under Grants Nos. MR2-995, MOR2-1033 and ME-2527.

## References

- [1] H. Cao, in: *Progress in Optics*, edited by E. Wolf, Vol. 45 (North-Holland, Amsterdam, 2003).
- [2] F. J. P. Schuurmans, D. Vanmaekelbergh, J. van de Lagemaat, and A. Lagendijk, *Science* **284**, 141 (1999).
- [3] H. Elhouichet, S. Daboussi, H. Ajlani, et al., *J. Lumin.* **113**, 329 (2005).
- [4] N. T. Bagraev and V. V. Romanov, *Semiconductors* **39**, 1131 (2005).
- [5] V. M. Konnov, N. N. Loiko, Yu. G. Sadof'ev, A. S. Trushin, and E. I. Makhov, *Semiconductors* **36**, 1215 (2002).
- [6] J. C. Phillips, *J. Appl. Phys.* **76**, 5896 (1994).
- [7] G. M. Williams, P. C. Becker, N. Edelstein, L. A. Boatner, and M. M. Abraham, *Phys. Rev. B* **40**, 1288 (1989).
- [8] J. Dexpert-Ghys, R. Mauricot, and M. D. Faucher, *J. Lumin.* **69**, 203 (1996).